International Journal of Offshore and Coastal Engineering
Vol.9 | No. 2 | pp. 16 – 32 | November 2025
e-ISSN: 2580-0914

Submitted: May 9, 2025 | Revised: July 4, 2025 | Accepted: August 15, 2025

Study Of Water Distribution Patterns and Temperature Changes in Waters Around Power Plant (Case Study of PLTU Tanjung Jati B Unit 5 & 6)

Fajar Lemanza Djazuli[a,*], Mukthasor and Shade Rahmawati

[a)] Departement of Ocean Engineering, Sepuluh Nopember Institute of Technology, Surabaya, Indonesia
*Corresponding author: anza.fajar@gmail.com

ABSTRACT

Sea cooling discharge refers to heated wastewater produced during the operational of a Steam Power Plant (PLTU). This effluent is typically discharged into the sea via an ocean outfall, a process that can significantly impact the surrounding marine environment and ecosystems. One of the primary consequences of this discharge is the elevation of seawater temperature in the vicinity of the outfall. This study aims to analyze the distribution patterns and temperature increases of seawater around the ocean outfall of Tanjung Jati B Power Plant Units 5 & 6. Numerical modeling was conducted using the Delft3D software, employing both the FLOW and WAVE modules to simulate the dispersion of thermal effluent and to assess temperature variations under different environmental conditions. The simulation results show that, during the west monsoon, the dispersion of thermal effluent predominantly extends toward the northeast, while during the east monsoon, the dispersion is mainly directed toward the west, northwest, and north. These findings underscore the significant influence of ocean currents and waves on the distribution of thermal effluent. Additionally, the maximum observed temperature increases of the thermal effluent reached 9°C, with the average area experiencing a temperature rise greater than 2°C measured at 932.16 m² during the west monsoon and 1,487.62 m² during the east monsoon, when comparing the 2024 dispersion pattern to the baseline seawater temperature in 2015. To mitigate the spread of thermal effluent, three alternative solutions are proposed: (1) extending the outfall structure, (2) evaluating and optimizing the design of the existing outfall. There are several potential approaches to minimize the dispersal of thermal wastewater, but further study is required to evaluate the effectiveness of these solutions.

Keywords: ***Thermal Water, PLTU, Delft 3D***

1. INTRODUCTION

As one of the world's largest archipelagic countries and the fourth most populous nation, Indonesia naturally requires an adequate and reliable supply of electrical energy. In Indonesia, steam power plants are predominantly utilized, owing to their high efficiency and the abundant availability of fuel sources domestically [1].

One of the crucial components that must be provided for sufficiently large-scale steam power plant is water. Water is used to condense the residual steam that has been utilized and to discharge water within the condenser, thereby enabling the power plant's cycle to operate properly and efficiently. Consequently, a substantial water source is essential for its operation [2]. To meet this demand, steam power plant commonly utilize seawater in their operations. In practice, the seawater used in a steam power plant is generally drawn through an intake channel, circulated into the plant for use, and subsequently discharged back into the sea after utilization [3]. The resulting waste—known as thermal effluent (power plant discharge)—exhibits significantly higher temperatures compared to natural seawater, due to its prior use in the power generation process.

One of the impacts arising from the discharge of thermal effluent is the increase in water temperature. According to the Indonesian Ministry of Environment and Forestry (Kementerian Lingkungan Hidup dan Kehutanan), as stipulated in Ministerial Decree (KEP-MENLH RI) No. 51/2004 regarding effluent water quality standards for coral reef ecosystems, the permissible increase in water temperature is defined as less than 2ºC above the natural temperature of the waters. This regulation is necessary because a substantial rise in water temperature can disrupt marine ecosystems, including fish and coral reefs.

This study aims to investigate the distribution patterns of thermal effluent and the temperature increase in seawater resulting from thermal effluent, both prior to and following

the operation of Tanjung Jati B Power Plant Units 5 & 6. This research is conducted to determine the distribution patterns of thermal effluent and to analyze the impact of temperature increases attributable to the discharge from Tanjung Jati B Power Plant Units 5 & 6.

2. BASIC THEORY

2.1 Tanjung Jati B Power Plant unit 5 & 6

Steam Power Plant (PLTU) is a power plant which uses dry steam to move turbine blades as a driving tool [1].

Figure 1. Location of Tanjung Jati B unit 5 & 6 Power Plant in Kembang District, Jepara Regency, Central Java

The case study of this study is a Tanjung Jati B Power Plant Units 5 & 6. This Steam Power Plant is one of the power plants is located on the island of Java, specifically in Kembang Subdistrict, Jepara Regency, Central Java. This power plant generates an electricity supply of 4 x 710 MW Gross or 4 x 660 MW Net. Its total capacity currently contributes approximately 12% of the overall electricity demand in the Java–Bali region. At present, Tanjung Jati B Power Plant has additional energy supply from two new units, namely Units 5 & 6, with a capacity of 2 x 1,070 MW.

2.2 Outfall Canal

Outfall is one of the infrastructural components of a steam power plant that functions as the discharge channel for thermal effluent or residual water from the plant's boiler operations to the sea [4]. In addition to serving as a conduit, the outfall also functions to reduce the temperature of the thermal effluent, which tends to be high. Generally, PLTUs employ an open outfall canal system (in the form of a canal) that discharges directly into the sea.

2.3 Thermal Effluent (Thermal Water)

Thermal effluent refers to hot wastewater from the operations of steam power plants. Typically, thermal effluent exhibits relatively high temperatures, ranging between 35ºC and 40ºC [4]. According to the Regulation of the State Minister of Environment No. 08 of 2009 (Peraturan Menteri Negara LH No.08 Tahun 2009) regarding "Wastewater Quality Standards for Thermal Power Plant Businesses and/or Activities," the maximum allowable temperature for effluent discharged by steam power plant is 40ºC. However, with respect to the permissible increase in seawater temperature, Ministerial Decree KEP-MENLH RI No. 51/2004 on effluent quality standards for coral reef ecosystems stipulates that the allowable temperature increase in the water is less than 2ºC (<2ºC). At the study location, the natural seawater temperature is approximately 29.5ºC, such a significant temperature difference is expected to cause impacts and exert influence on the surrounding ecosystem.

2.4 Sea Current and Sea Wave

Sea currents refer to the horizontal and vertical movement of water masses from one location to another, occurring continuously. Sea currents have both direction and velocity within a given marine area, thereby forming specific movement patterns within that region [5]. Meanwhile, sea waves are oscillations of matter that transfer energy through a propagating movement using seawater as the medium of transmission [6].

In this study, sea currents and sea waves constitute key factors observed in relation to the movement, direction, and distribution patterns of thermal effluent in the waters surrounding Tanjung Jati B Power Plant Units 5 and 6.

3. METHODOLOGY

3.1 Study Prosedure

A literature review was conducted utilizing various journals and books relevant to this study to serve as references for the completion of this research. The literature employed in this study includes books, scholarly journals, and previous theses that are similar in scope and subject matter to the present research.

3.2 Data Collection

The data utilized in this study are secondary data obtained from various sources to construct simulation models that accurately reflect actual field conditions. This research considers two seasonal conditions: the West Monsoon Wind condition and the East Monsoon Wind condition. The following presents a detailed description of the data employed in this study.

Table 1. Data Needed to Simulate the Model

Conditions	Description	Value

The West Monsoon Wind (March)	Averaged Natural Seawater Temperature	29,53 °C
	Significant Wave Height (SWH)	0,5422 m
	Peak Period (Tp)	3,65 s
	Direction (Nautical)	290°
The East Monsoon Wind (June)	Averaged Natural Seawater Temperature	29,87 °C
	Significant Wave Height (SWH)	0,658
	Peak Period (Tp)	3,91 s
	Direction (Nautical)	70°

In this study, three variations of thermal water temperature were simulated, namely the minimum, average, and maximum thermal water temperatures, assuming a discharge rate of 91.667 m³/s. The following table presents the temperature data of the waste heat water used in the model.

Table 2. Data Variations of Thermal Water Temperature

Conditions	Variations	Value
The West Monsoon Wind (March)	Minimum Temperature	32,10 °C
	Average Temperature	35,55 °C
	Maximum Temperature	37,84 °C
The East Monsoon Wind (June)	Minimum Temperature	30,33 °C
	Average Temperature	34,38 °C
	Maximum Temperature	38,28 °C

In addition to the aforementioned data, bathymetric data of the power plant waters area were utilized in this simulation. The following figure illustrates the bathymetry of the Tanjung Jati B Power Plant units 5 and 6 waters.

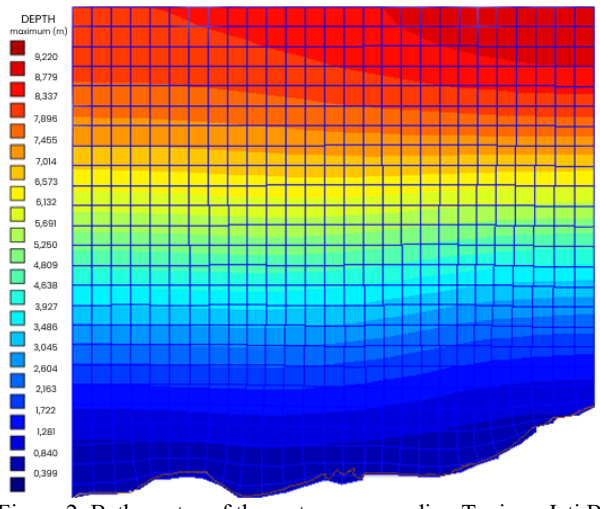

Figure 2. Bathymetry of the waters surrounding Tanjung Jati B Power Plant units 5 and 6 presented in a visual grid.

The average depth of the waters surrounding the power plant tends to be shallow, with a maximum depth of approximately 9 meters within a 3 km radius from the Jepara coastline.

The above-mentioned data were predominantly obtained from several official sources that provide such information. For instance, water temperature data were sourced from Surftemp.net, wave data from the ECMWF website, and bathymetric data from Ina-Geospatial. Only the thermal water temperature data represent primary data, which were collected directly from the measurement stations at Tanjung Jati B Power Plants units 5 and 6

3.3 Modeling Simulation

In this study, the simulation of the dispersion pattern resulting from the discharge of steam water from Tanjung Jati B Power Plant units 5 and 6 was conducted using the Delft3D software, which integrates two of its modules: Delft3D-FLOW, employed to simulate marine currents, and Delft3D-WAVE, used to simulate sea waves. This combined approach enables comprehensive hydrodynamic and wave modeling to accurately represent the environmental conditions affected by the thermal discharge

3.4 Modeling Validation

In this study, model validation against real field conditions was performed by calculating the error difference between tidal and ocean current results generated by the Delft3D model and observed data obtained from BIG.id for tidal measurements and the AMDAL report of Tanjung Jati B Power Plants units 5 and 6 for ocean current data.

The error calculation method employed was the *Root Mean Square Error* (RMSE), which quantifies the difference between actual observed values and model-predicted values [7]. The equation used is as follows.

$$RMSE = \sqrt{\frac{\sum_{t=1}^{n}(At-Ft)^2}{n}} \quad (4)$$

Where *At* represents the actual data at time, *Ft* denotes the modeled data at time, and *n* is the total number of data points or time periods.

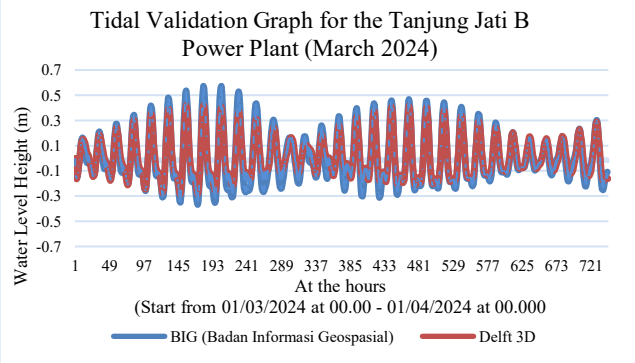

Figure 3. Tidal Validation Graph of Tanjung Jati B Power Plants Waters Units 5 & 6 in March 2024

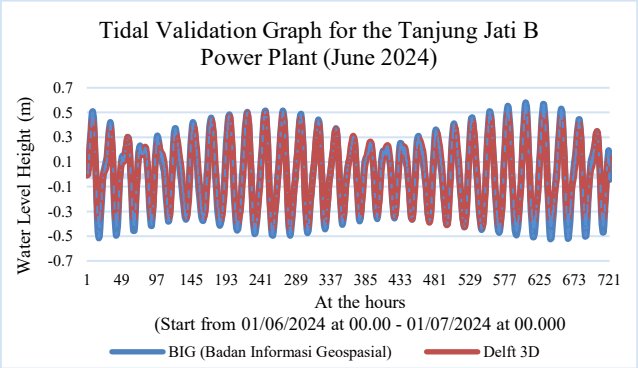

Figure 4. Tidal Validation Graph of Tanjung Jati B Power Plants Waters Units 5 & 6 in June 2024

After computation, the percentage error in tidal prediction was found to be 9% for the month of March (West Monsoon), while for the month of June (East Monsoon), the percentage error was 7%.

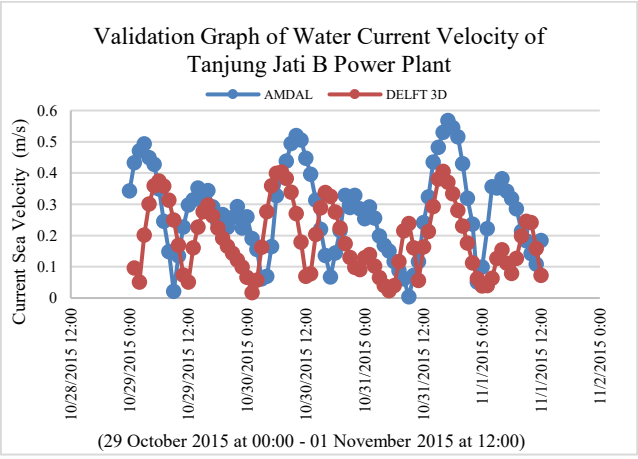

Figure 5. Validation Graph of Water Current Velocity of Tanjung Jati B Power Plant

For the current validation, an error percentage of 39% was obtained based on the comparison between the model results and the AMDAL data from Tanjung Jati B Power Plant units 5 and 6 for the corresponding time period. The following figure presents the validation graph of the current data in the waters surrounding Tanjung Jati B Power Plant units 5 and 6.

4. EVALUATION AND DISCUSSION

4.1 Simulation Model Creation

In the Delft3D software, it is necessary to develop a grid model and incorporate other relevant elements specific to the study area to ensure that the simulation accurately represents the field conditions. Furthermore, grid generation serves to confine the simulation domain within a defined spatial extent, facilitating focused and efficient model computations. The following figure illustrates the grid model employed in this study.

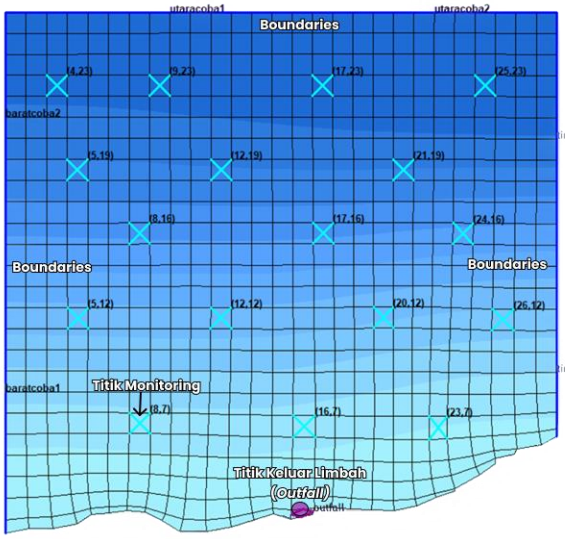

Figure 6. Grid model used for simulation of Tanjung Jati B Power Plant units 5 & 6

The grid model depicted in Figure 5 consists of 29 cells in the M-direction and 27 cells in the N-direction, corresponding to a physical field scale of approximately 2.9 km vertically and 3.3 km horizontally. These spatial extents are constrained by the model boundaries on the right, left, and top sides, which serve as the limits of the study domain. In addition to the grid, several points with distinct functions have been incorporated into the model. These include discharge points, which act as the initial locations of the waste heat water release within the simulation, and monitoring points, which serve as specific locations for observation and data collection throughout the modeling process.

4.2 Thinning Wall Thickness Analysis

Table 3. Time of Simulation and Duration in March and June

Description	March (West Monsoon)	June (East Monsoon)
Simulation Date	01 March 2024	01 June 2024
Start Time	01 March 2024	01 June 2024
Stop Time	01 April 2024	01 July2024
Simulation Duration	31 days	30 days

During the simulation preparation phase, all necessary input data were incorporated to enable the simulation process. These inputs included wave data, water temperature data, thermal water temperature data, discharge flow rates, and other relevant parameters required by the software to accurately simulate the hydrodynamic conditions of the waters surrounding Tanjung Jati B Power Plant units 5 and 6. Following the data input, the simulation duration was

configured. Table 1 summarizes the simulation time frames conducted for March (West Monsoon) and June (East Monsoon) conditions.

4.3 Distribution Pattern of Thermal Water Temperature from Tanjung Jati B Power PlantUnits 5 & 6

Following the simulation of the model, an analysis of the temperature distribution pattern in the waters surrounding Power Plant Tanjung Jati B units 5 and 6 was conducted for March (West Monsoon) and June (East Monsoon) with three thermal water temperature variations. The simulation results examined in this study correspond to four tidal conditions: Lowest Ebb, Highest Flood, Ebb to Flood transition, and Flood to Ebb transition. The following sections present the simulation outcomes for each respective season.

4.3.1 West Monsoon Condition (March)

1. Minimum Temperature Variations

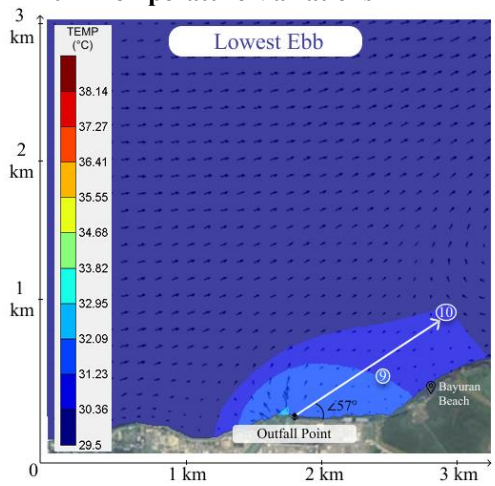

Figure 7. Thermal Water Temperature Distribution Pattern at Lowest Ebb Condition (March 7, 2024, 03:00 WIB)

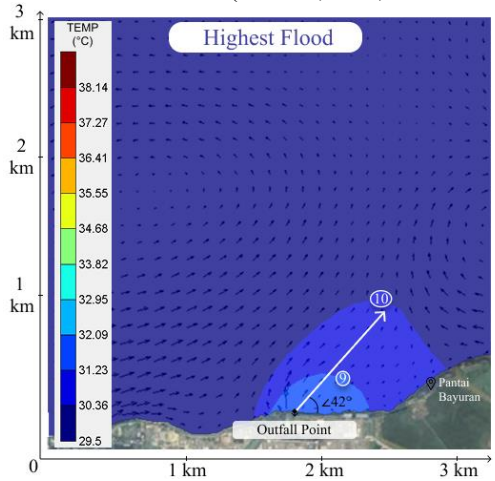

Figure 8. Thermal Water Temperature Distribution Pattern at Highest Flood Condition (March 7, 2024, 11:00 WIB)

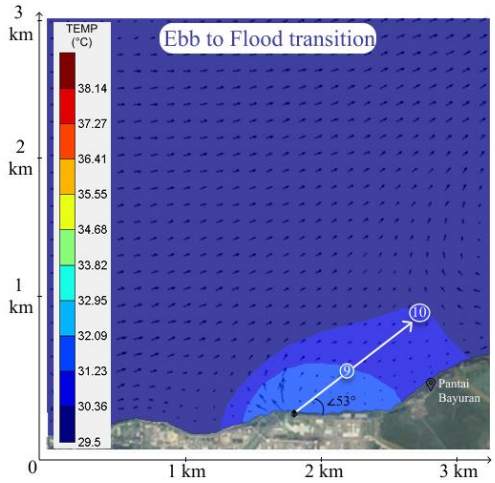

Figure 9. Thermal Water Temperature Distribution Pattern at Ebb to Flood transition Condition (March 22, 2024, 04:00 WIB)

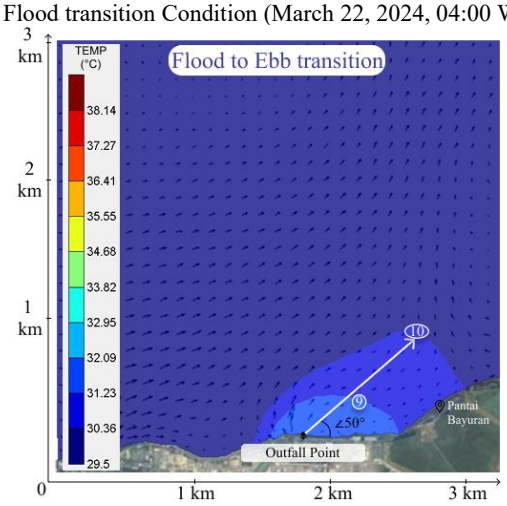

Figure 10. Thermal Water Temperature Distribution Pattern at Flood to Ebb transition Condition (March 22, 2024, 16:00 WIB)

Figures 7 and Table 4 illustrate that the highest temperature dispersion at the lowest ebb condition ranges from 31,23 °C to 32,09 °C, at point number 9. with the maximum dispersion distance approximately 1.550 meters from the outfall mouth. The waste heat water plume disperses toward the northeast direction (θ = 57°). During the highest flood condition at Figures 8 and Table 4, the peak temperature range remains consistent with the lowest ebb condition; however, the maximum dispersion distance slightly decreases to approximately 1.250 meters, with the plume spreading toward the northeast (θ = 42°).

Similarly, Figures 9 and Table 5 show that at the ebb-to-flood transition, the highest temperature dispersion remains between 31,23 °C and 32,09 °C, at point number 9, with a maximum dispersion distance of about 1.420 meters from the outfall mouth and a northeastward plume direction (θ = 53°). In the flood-to-ebbing transition at Figures 10 and Table 5, the temperature distribution is comparable, with the maximum dispersion distance around 1.310 meters from the outfall mouth, and the plume extends to the northeast at an

angle of approximately 50°.

Table 4. Area of Thermal Water Dispersion and Maximum Dispersion Distance under Lowest Ebb and Highest Flood Conditions

Radius Point	Temperature (°C)	Lowest Ebb		Highest Flood	
		Area (m^2)	Distance (m)	Area (m^2)	Distance (m)
1	39- 38,14	-	-	-	-
2	38,14 - 37,27	-	-	-	-
3	37,27 - 36,41	-	-	-	-
4	36,41 - 35,55	-	-	-	-
5	35,55 - 34,68	-	-	-	-
6	34,68 - 33,82	-	-	-	-
7	33,82 - 32,95	-	-	-	-
8	32,95 - 32,09	-	-	-	-
9	32,09 - 31,23	414,8	920	188,3	612
10	31,23 - 30,36	635,5	1.550	660,1	1.250

Table 5. Area of Thermal Water Dispersion and Maximum Dispersion Distance under Ebb to Flood transition and Flood to Ebb transition Conditions

Radius Point	Temperature (°C)	Ebb to Flood transition		Flood to Ebb transition	
		Area (m^2)	Distance (m)	Area (m^2)	Distance (m)
1	39- 38,14	-	-	-	-
2	38,14 - 37,27	-	-	-	-
3	37,27 - 36,41	-	-	-	-
4	36,41 - 35,55	-	-	-	-
5	35,55 - 34,68	-	-	-	-
6	34,68 - 33,82	-	-	-	-
7	33,82 - 32,95	-	-	-	-
8	32,95 - 32,09	-	-	-	-
9	32,09 - 31,23	382	840	263	745
10	31,23 - 30,36	622,3	1.420	578,3	1.310

2. Average Temperature Variations

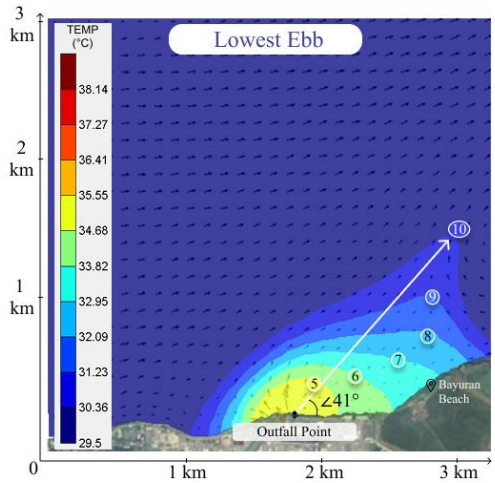

Figure 11. Thermal Water Temperature Distribution Pattern at Lowest Ebb Condition (March 7, 2024, 03:00 WIB)

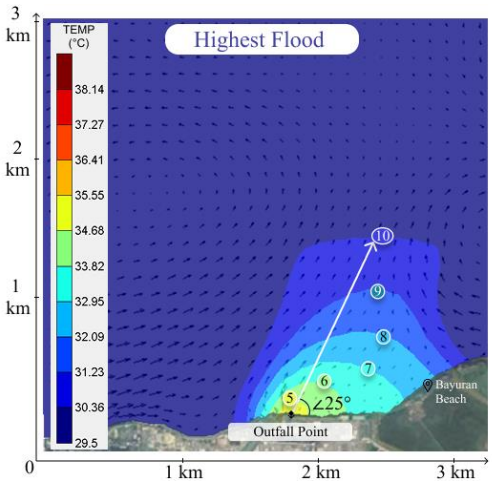

Figure 12. Thermal Water Temperature Distribution Pattern at Highest Flood Condition (March 7, 2024, 11:00 WIB)

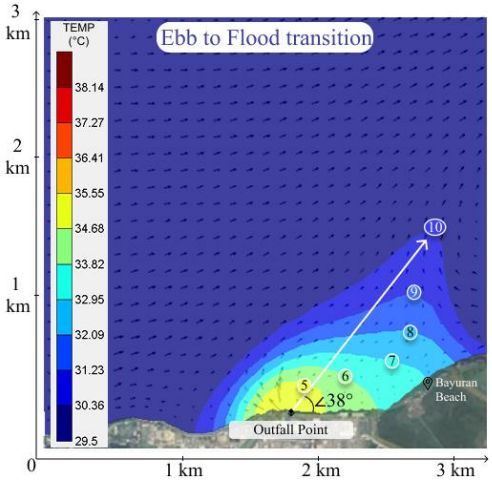

Figure 13. Thermal Water Temperature Distribution Pattern at Ebb to Flood transition Condition (March 22, 2024, 04:00 WIB)

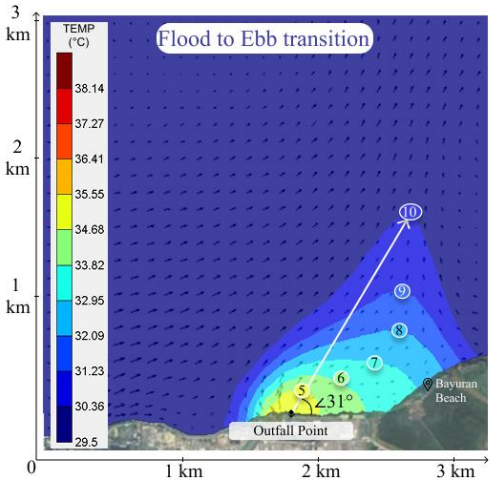

Figure 14. Thermal Water Temperature Distribution Pattern at Flood to Ebb transition Condition (March 22, 2024, 16:00 WIB)

In Figure 11 and Table 6, the highest temperature distribution under both lowest ebb and highest flood conditions was observed in the range of 34,68 °C to 35,55 °C, at point number 5. During the lowest ebb condition, the maximum extent of the thermal plume reached approximately 1.964 m from the outfall, with the dispersion direction oriented toward the northeast (θ = 41°). Conversely, under the highest flood condition, as shown in Figure 12 and Table 6, the furthest extent of dispersion was about 1.785 m, with the plume also directed northeastward (θ = 25°).

Furthermore, Figure 13 and Table 7 indicate that the highest temperature dispersion under ebb-to-flood and flood-to-ebb transition conditions remained within the same temperature range as previously mentioned. In the ebb-to-flood transition, the maximum dispersion distance was approximately 1.850 m from the outfall, with a northeastward direction (θ = 38°). In contrast, Figure 104 and Table 7 show that, during the flood-to-ebb transition, the furthest plume extent was about 1.820 m, with a northeastward dispersion angle of 27°.

Table 6. Area of Thermal Water Dispersion and Maximum Dispersion Distance under Lowest Ebb and Highest Flood Conditions

Radius Point	Temperature (°C)	Lowest Ebb		Highest Flood	
		Area (m^2)	Distance (m)	Area (m^2)	Distance (m)
1	39- 38,14	-	-	-	-
2	38,14 - 37,27	-	-	-	-
3	37,27 - 36,41	-	-	-	-
4	36,41 - 35,55	-	-	-	-
5	35,55 - 34,68	158,4	470	28	230
6	34,68 - 33,82	198,4	850	106,6	475
7	33,82 - 32,95	254,2	1.260	236,3	900
8	32,95 - 32,09	270,2	1.485	287,6	1.150
9	32,09 - 31,23	313,5	1.635	376,8	1.315
10	31,23 - 30,36	485	1.964	706	1.785

Table 7. Area of Thermal Water Dispersion and Maximum Dispersion Distance under Ebb to Flood transition and Flood to Ebb transition Conditions

Radius Point	Temperature (°C)	Ebb to Flood transition		Flood to Ebb transition	
		Area (m^2)	Distance (m)	Area (m^2)	Distance (m)
1	39- 38,14	-	-	-	-
2	38,14 - 37,27	-	-	-	-
3	37,27 - 36,41	-	-	-	-
4	36,41 - 35,55	-	-	-	-
5	35,55 - 34,68	122,2	360	73	305
6	34,68 - 33,82	184,2	690	136	600
7	33,82 - 32,95	258,1	1.125	234,5	1.000
8	32,95 - 32,09	258,6	1.325	263,3	1.230
9	32,09 - 31,23	309,8	1.460	311,7	1.360
10	31,23 - 30,36	511,7	1.850	546,4	1.820

3. Maximum Temperature Variations

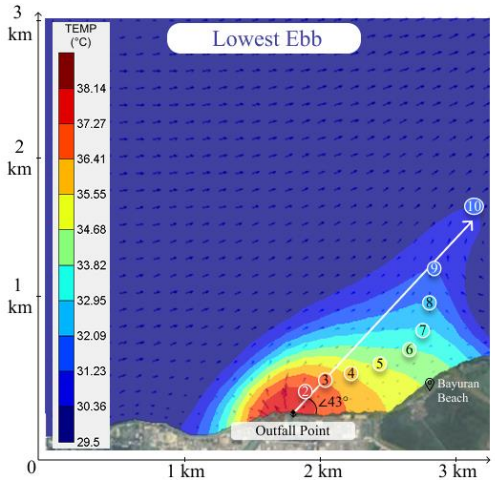

Figure 15. Thermal Water Temperature Distribution Pattern at Lowest Ebb Condition (March 7, 2024, 03:00 WIB)

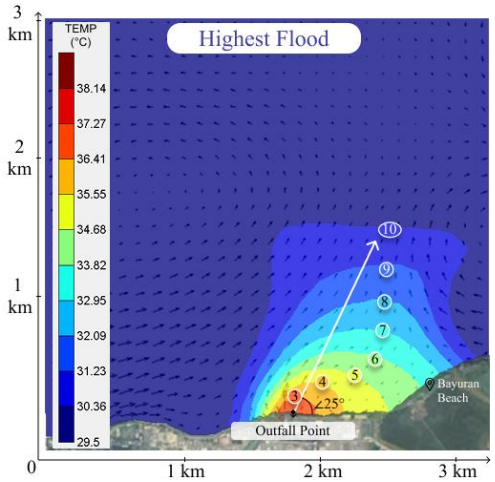

Figure 16. Thermal Water Temperature Distribution Pattern at Highest Flood Condition (March 7, 2024, 11:00 WIB)

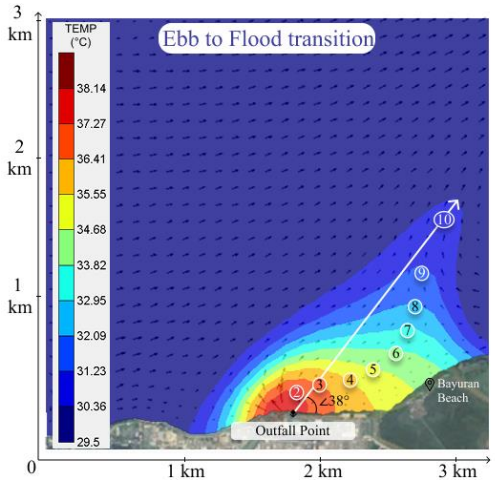

Figure 17. Thermal Water Temperature Distribution Pattern at Ebb to Flood transition Condition (March 22, 2024, 04:00 WIB)

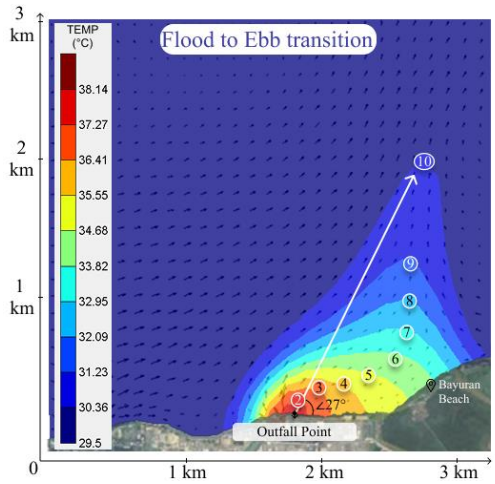

Figure 18. Thermal Water Temperature Distribution Pattern at Flood to Ebb transition Condition (March 22, 2024, 16:00 WIB)

Figures 15 and Table 8 show that the highest temperature distribution at the lowest ebb condition ranges from 37,27 °C to 38,14 °C, at point number 2, with the maximum dispersion distance approximately 2.175 meters from the outfall mouth. The waste heat water plume spreads toward the northeast direction (θ = 43°). In contrast, at the highest flood condition at Figures 16 and Table 8 the highest temperature distribution ranges from 36,91 °C to 37,27 °C, at point number 3, with a maximum dispersion distance of about 1.930 meters, also directed toward the northeast (θ = 25°).

Furthermore, Figures 17 and Table 9 illustrate that during the ebb-to-flood transition, the highest temperature distribution remains between 37,27 °C and 38,14 °C, at point number 2. The maximum dispersion distance is approximately 2.130 meters from the outfall mouth, with the waste heat plume spreading northeastward (θ = 38°). This dispersion pattern during the ebb-to-flood transition is similar to that observed at the lowest ebb condition. Finally, in the Figures 18 and Table 9, the flood-to-ebb transition condition exhibits the highest temperature distribution within the same range of 37,27 °C to 38,14 °C, at point number 2, with the maximum dispersion distance extending to about 2.240 meters. The plume direction remains toward the northeast, tending toward north (θ = 27°).

Table 8. Area of Thermal Water Dispersion and Maximum Dispersion Distance under Lowest Ebb and Highest Flood Conditions

Radius Point	Temperature (°C)	Lowest Ebb		Highest Flood	
		Area (m^2)	Distance (m)	Area (m^2)	Distance (m)
1	39- 38,14	-	-	-	-
2	38,14 - 37,27	86,7	295	-	-
3	37,27 - 36,41	113,6	445	39	282
4	36,41 - 35,55	142,5	725	81,7	468
5	35,55 - 34,68	169	1.030	151,3	765
6	34,68 - 33,82	197	1.260	201,5	1.050
7	33,82 - 32,95	198,5	1.405	221,2	1.200
8	32,95 - 32,09	230	1.515	261,4	1.280
9	32,09 - 31,23	285,2	1.630	378,2	1.545
10	31,23 - 30,36	535	2.175	775,4	1.930

Table 9. Area of Thermal Water Dispersion and Maximum Dispersion Distance under Ebb to Flood transition and Flood to Ebb transition Conditions

Radius Point	Temperature (°C)	Ebb to Flood transition		Flood to Ebb transition	
		Area (m^2)	Distance (m)	Area (m^2)	Distance (m)
1	39- 38,14	-	-	-	-
2	38,14 - 37,27	59,3	255	27,6	190
3	37,27 - 36,41	89,6	390	71,4	360
4	36,41 - 35,55	139	650	101,8	585
5	35,55 - 34,68	175	970	156,8	900
6	34,68 - 33,82	195,8	1.215	178,2	1.125
7	33,82 - 32,95	192,3	1.340	192,3	1.250
8	32,95 - 32,09	214	1.4250	201,3	1.345
9	32,09 - 31,23	296,6	1.570	294	1.530
10	31,23 - 30,36	551,6	2.130	655	2.240

4.3.2 East Monsoon Condition (June)

1. Minimum Temperature Variations

Figures 19 and 20 do not show any discernible temperature distribution patterns in the waters surrounding the power plant. This is attributed to the very small temperature difference between the ambient water and the waste heat discharge, which is less than 1 °C, resulting in no significant temperature variations or distribution patterns in the water.

Based on the simulation results, it can be concluded that the dispersion pattern of thermal water is strongly influenced by ocean currents and wave dynamics. This is evident from the significant impact of the West and East Monsoon conditions on the dispersion pattern of the thermal discharge from Tanjung Jati B Power Plant units 5 and 6.

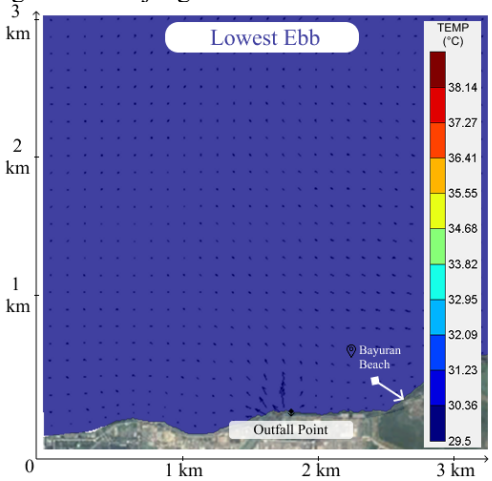

Figure 19. Thermal Water Temperature Distribution Pattern at Lowest Ebb Condition (June 27, 2024, 15:00 WIB)

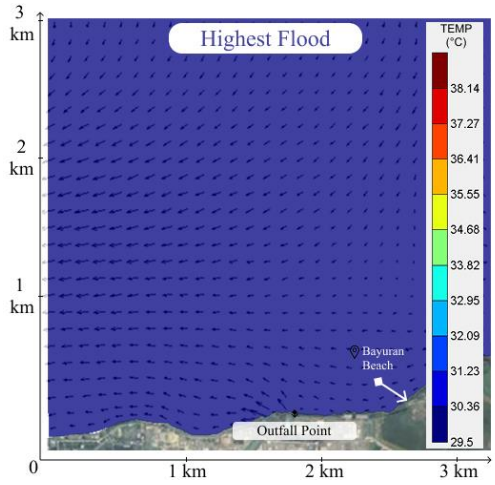

Figure 20. Thermal Water Temperature Distribution Pattern at Highest Flood Condition (June 26, 2024, 15:00 WIB)

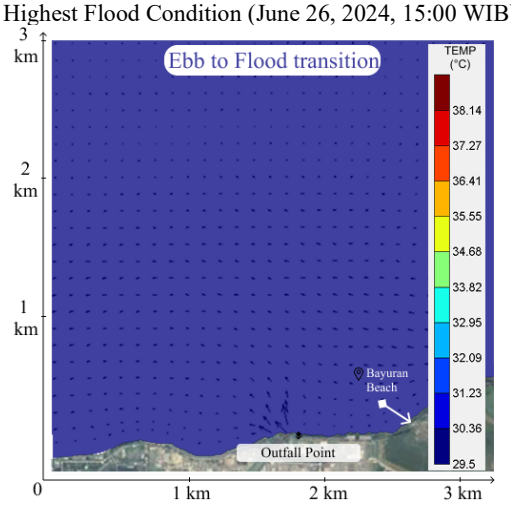

Figure 21. Thermal Water Temperature Distribution Pattern at Ebb to Flood transition Condition (June 2, 2024, 19:00 WIB)

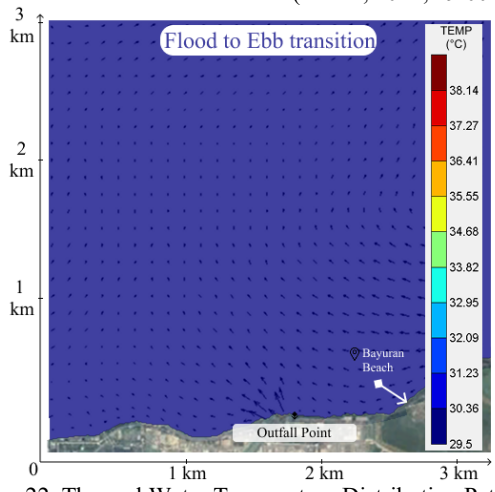

Figure 22. Thermal Water Temperature Distribution Pattern at Flood to Ebb transition Condition (June 3, 2024, 11:00 WIB)

2. Average Temperature Variations

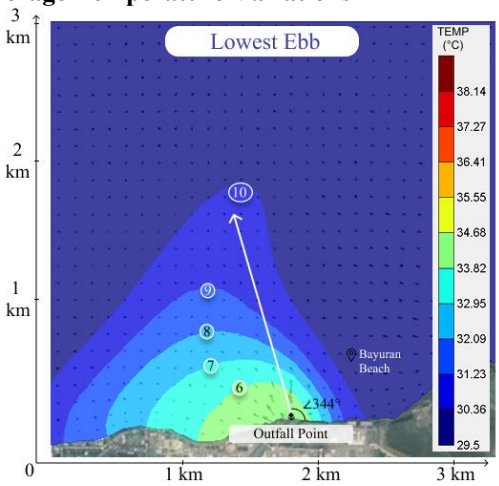

Figure 23. Thermal Water Temperature Distribution Pattern at Lowest Ebb Condition (June 27, 2024, 15:00 WIB)

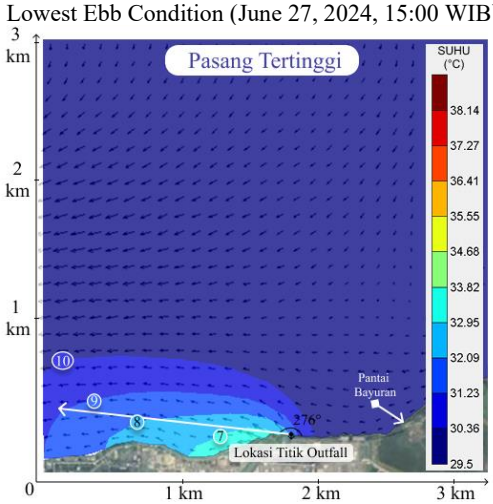

Figure 24. Thermal Water Temperature Distribution Pattern at Highest Flood Condition (June 26, 2024, 15:00 WIB)

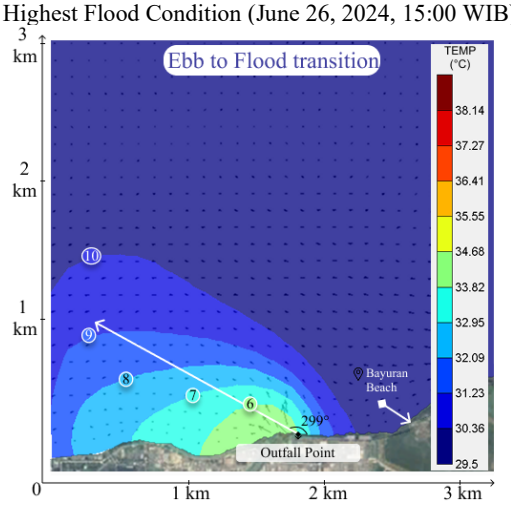

Figure 25. Thermal Water Temperature Distribution Pattern at Ebb to Flood transition Condition (June 2, 2024, 19:00 WIB)

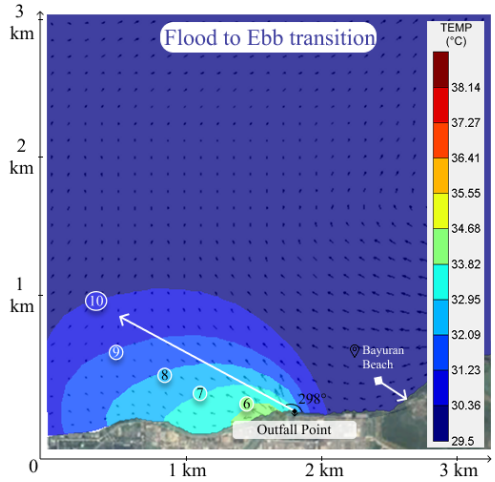

Figure 26. Thermal Water Temperature Distribution Pattern at Flood to Ebb transition Condition (June 3, 2024, 11:00 WIB)

Figures 23 and Table 10 illustrate that the highest temperature distribution at the lowest ebb condition ranges from 33,82 °C to 34,68 °C, at point number 6, with a maximum dispersion distance of approximately 1.890 meters from the outfall mouth. The waste heat water plume disperses toward the north-northwest direction (θ = 344°). In contrast, under the highest flood condition at Figures 24 and Table 10, the peak temperature distribution ranges from 32,95 °C to 33,82 °C, at point number 7, with a maximum dispersion distance of about 1.870 meters, and the plume spreads toward the west (θ = 276°). These two conditions exhibit a notably distinct dispersion direction.

Furthermore, Figures 25 and Table 11 show that during the ebb-to-flood transition, the highest temperature distribution remains between 33,82 °C and 34,68 °C, at point number 6. The maximum dispersion distance extends to approximately 2.120 meters from the outfall mouth, with the thermal plume spreading northwestward (θ = 299°). The highest temperature dispersion during the flood-to-ebb transition at Figures 26 and Table 11 is similar to that of the ebb-to-flood transition, with a slightly reduced maximum extent of about 1.900 meters and a northwestward dispersion direction (θ = 307°).

Table 10. Area of Thermal Water Dispersion and Maximum Dispersion Distance under Lowest Ebb and Highest Flood Conditions

Radius Point	Temperature (°C)	Lowest Ebb		Highest Flood	
		Area (m^2)	Distance (m)	Area (m^2)	Distance (m)
1	39- 38,14	-	-	-	-
2	38,14 - 37,27	-	-	-	-
3	37,27 - 36,41	-	-	-	-
4	36,41 - 35,55	-	-	-	-
5	35,55 - 34,68	-	-	-	-
6	34,68 - 33,82	242,1	700	-	-
7	33,82 - 32,95	315,7	1.080	80,1	700
8	32,95 - 32,09	378,2	1.380	200,6	1.300
9	32,09 - 31,23	558	1.680	393,5	1.780
10	31,23 - 30,36	1.038	1.890	530,5	1.870

Table 11. Area of Thermal Water Dispersion and Maximum Dispersion Distance under Ebb to Flood transition and Flood to Ebb transition Conditions

Radius Point	Temperature (°C)	Ebb to Flood transition		Flood to Ebb transition	
		Area (m^2)	Distance (m)	Area (m^2)	Distance (m)
1	39- 38,14	-	-	-	-
2	38,14 - 37,27	-	-	-	-
3	37,27 - 36,41	-	-	-	-
4	36,41 - 35,55	-	-	-	-
5	35,55 - 34,68	-	-	-	-
6	34,68 - 33,82	178,5	665	44	420
7	33,82 - 32,95	298,4	1.190	197,3	920
8	32,95 - 32,09	465	1.650	277,6	1.360
9	32,09 - 31,23	588,6	1.820	487,8	1.700
10	31,23 - 30,36	895,5	2.120	767,8	1.900

3. Maximum Temperature Variations

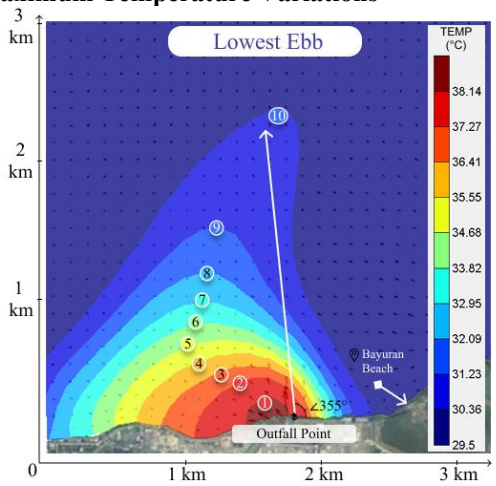

Figure 27. Thermal Water Temperature Distribution Pattern at Lowest Ebb Condition (June 27, 2024, 15:00 WIB)

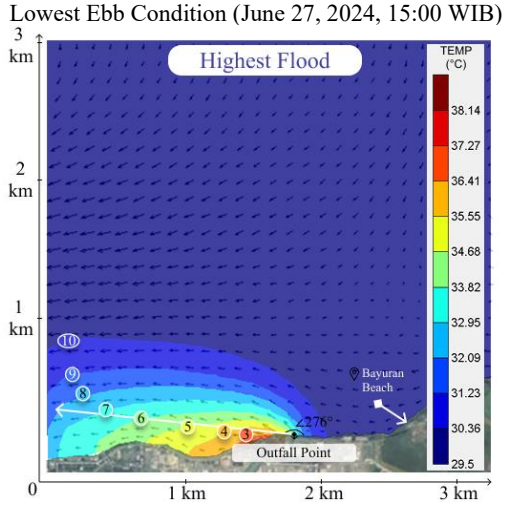

Figure 28. Thermal Water Temperature Distribution Pattern at Highest Flood Condition (June 26, 2024, 15:00 WIB)

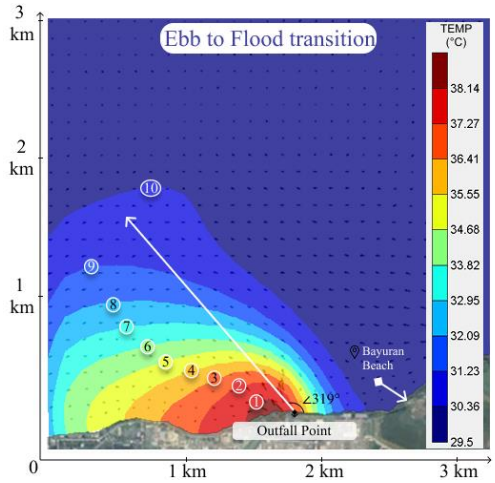

Figure 29. Thermal Water Temperature Distribution Pattern at Ebb to Flood transition Condition (June 2, 2024, 19:00 WIB)

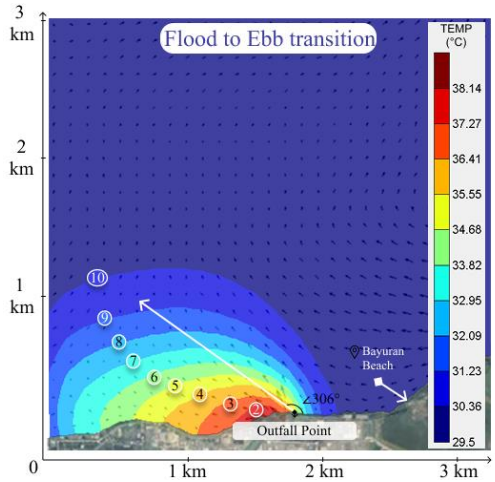

Figure 30. Thermal Water Temperature Distribution Pattern at Flood to Ebb transition Condition (June 3, 2024, 11:00 WIB)

Figures 27 and Table 12 show that the highest temperature distribution during the lowest ebb condition ranges from 38,14 °C to 39 °C, at point number 1, with the maximum dispersion distance approximately 2.400 meters from the outfall mouth. The thermal plume disperses toward the north (θ = 355°). In contrast, under the highest flood condition shown in Figure 28 and Table 12, the highest temperature distribution ranges from 36,41 °C to 37,27 °C, at point number 3, with a maximum dispersion distance of about 1.950 meters, and the plume disperses westward (θ = 276°).

Furthermore, Figures 29 and Table 13 illustrate that during the ebb-to-flood transition, the highest temperature distribution remains between 38,14 °C and 39 °C, at point number 1, with a maximum dispersion distance of approximately 2.305 meters from the outfall mouth. The plume disperses toward the northwest (θ = 319°). The temperature dispersion pattern during the flood-to-ebb transition at Figures 30 and Table 13 is similar to that of the ebb-to-flood condition; however, the highest temperature range narrows to 37,27 °C to 38,14 °C, at point number 2, with a maximum dispersion distance of around 1.985 meters, and the plume disperses toward the northeast (θ = 306°).

Table 12. Area of Thermal Water Dispersion and Maximum Dispersion Distance under Lowest Ebb and Highest Flood Conditions

Radius Point	Temperature (°C)	Lowest Ebb		Highest Flood	
		Area (m^2)	Distance (m)	Area (m^2)	Distance (m)
1	39- 38,14	48	310	-	-
2	38,14 - 37,27	185,8	690	-	-
3	37,27 - 36,41	175,7	925	28,5	415
4	36,41 - 35,55	168,2	1.120	73,7	730
5	35,55 - 34,68	200,7	1.290	104,5	1.050
6	34,68 - 33,82	234,2	1.455	152,2	1.440
7	33,82 - 32,95	297,8	1.625	215,4	1.710
8	32,95 - 32,09	356,7	1.740	215,5	1.805
9	32,09 - 31,23	498,4	1.800	260	1.850
10	31,23 - 30,36	1.230	2.400	436,7	1.950

Table 13. Area of Thermal Water Dispersion and Maximum Dispersion Distance under Ebb to Flood transition and Flood to Ebb transition Conditions

Radius Point	Temperature (°C)	Ebb to Flood transition		Flood to Ebb transition	
		Area (m^2)	Distance (m)	Area (m^2)	Distance (m)
1	39- 38,14	45,7	320	-	-
2	38,14 - 37,27	145,5	675	51,2	415
3	37,27 - 36,41	160	960	88,7	675
4	36,41 - 35,55	176,3	1.230	123	935
5	35,55 - 34,68	242,3	1.520	137,2	1.170
6	34,68 - 33,82	270,4	1.690	190	1.420
7	33,82 - 32,95	305,7	1.765	254,2	1.630
8	32,95 - 32,09	338,6	1.880	298	1.740
9	32,09 - 31,23	438,4	2.020	382,2	1.845
10	31,23 - 30,36	956,2	2.305	631,6	1.985

The simulation results indicate that the direction of ocean currents and wave dynamics exert a significant influence on the dispersion pattern of waste heat discharge.

4.4 Results of Thermal Water Temperature Changes at Tanjung Jati B Power Plant Units 5 & 6

Subsequently, an analysis was conducted on the temperature changes resulting from the waste heat discharge in the waters surrounding Tanjung Jati B Power Plant units 5 and 6 during March (West Monsoon) and June (East Monsoon), using the baseline water temperature data prior to the operation of units 5 and 6 in 2015. The simulation results in this study were observed under four temporal conditions: Lowest Ebb, Highest Flood, Ebb to Flood transition, and Flood to Ebb transition. The following sections present the simulation outcomes for each respective season.

4.4.1 West Monsoon Condition (March)

1. Minimum Temperature Variations

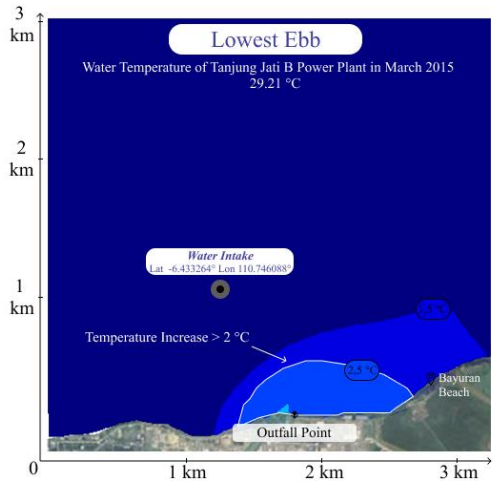

Figure 31. Increase in Thermal Water Temperature at Lowest Ebb Condition Compared to Ambient Water Temperature in 2015

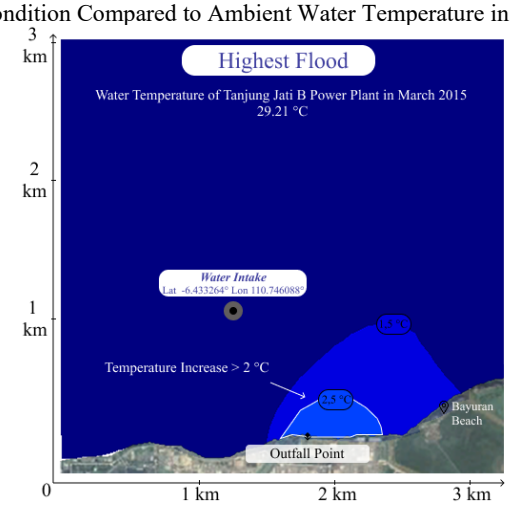

Figure 32. Increase in Thermal Water Temperature at Highest Flood Condition Compared to Ambient Water Temperature in 2015

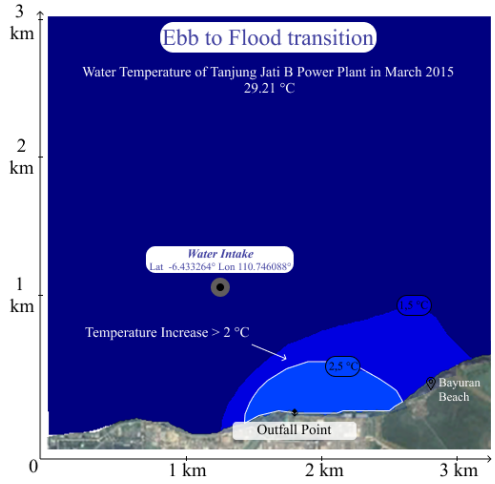

Figure 33. Increase in Thermal Water Temperature at Ebb to Flood Transisition Condition Compared to Ambient Water Temperature in 2015

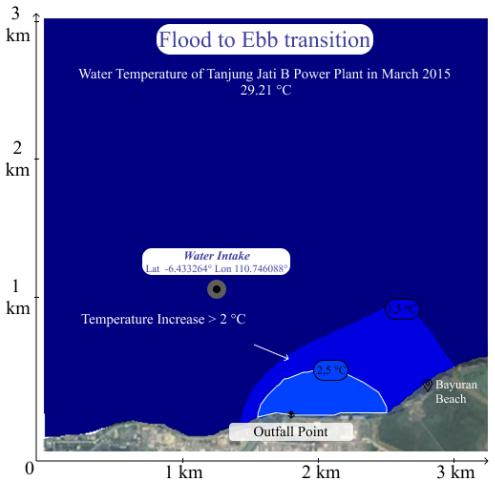

Figure 34. Increase in Thermal Water Temperature at Flood to Ebb Transition Condition Compared to Ambient Water Temperature in 2015

Under the lowest ebb condition with minimum waste heat temperature variation, as illustrated in Figure 31, the maximum temperature increase is approximately ±2,5 °C. The area of seawater experiencing a surface temperature rise exceeding 2 degrees Celsius (> 2°C) around the power plant is approximately 455 m², with the maximum dispersion distance reaching 920 meters from the outfall mouth. Similarly, under the highest flood condition at Figure 32, the maximum temperature increase remains approximately ±2,5 °C. The area affected by a surface temperature increase greater than 2°C is about 205 m², with a maximum dispersion distance of 612 meters from the outfall.

Furthermore, during the ebb-to-flood transition (Figure 33), the highest temperature increase is approximately ±2,5 °C, with the affected seawater area measuring approximately 400 m² and a maximum dispersion distance of 840 meters from the outfall mouth. Consistent with previous conditions, during the flood-to-ebb transition (Figure 34), the temperature increase remains around ±2.5 °C, though the affected area is smaller at approximately 280 m², with the maximum dispersion distance reaching 745 meters from the outfall mouth.

2. Average Temperature Variations

Under the lowest ebb condition (Figure 35), the maximum observed temperature increase reaches approximately ±6 °C. The area of seawater experiencing a surface temperature elevation greater than 2 °C (>2 °C) around the power plant is about 1.205 m², with the farthest extent of the temperature increase reaching 1.635 m from the outfall mouth. A significant contrast is evident during the highest flood condition (Figure 36), where the maximum temperature rise is similarly ±6 °C. However, the area with surface temperature increases exceeding 2 °C contracts to approximately 1.050 m², with a maximum dispersion

distance of 1.315 m from the outfall.

During the ebb-to-flood transition (Figure 4.38, left), the maximum temperature increase remains at ±6 °C. The affected surface area (where the increase exceeds 2 °C) is about 1.136 m², and the maximum dispersion distance is 1.460 m from the outfall mouth. Consistently, under the flood-to-ebb transition (Figure 4.38, right), the peak temperature rise is ±6 °C, with a slightly smaller affected area of 1.010 m² and a maximum extent of 1.360 m from the outfall.

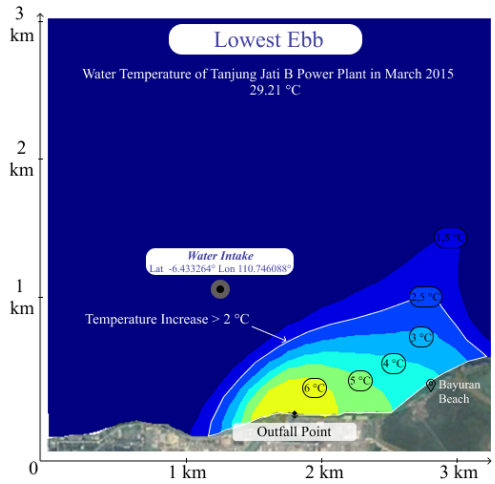

Figure 35. Increase in Thermal Water Temperature at Lowest Ebb Condition Compared to Ambient Water Temperature in 2015

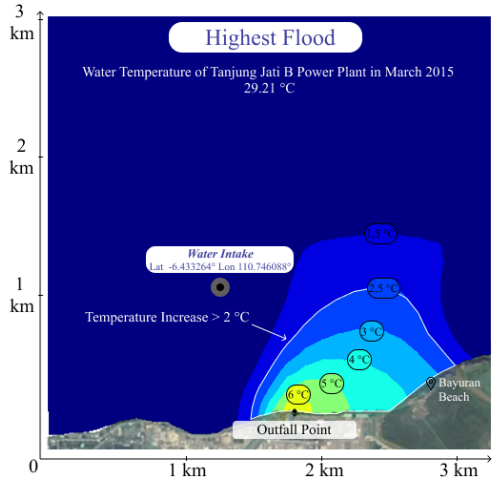

Figure 36. Increase in Thermal Water Temperature at Highest Flood Condition Compared to Ambient Water Temperature in 2015

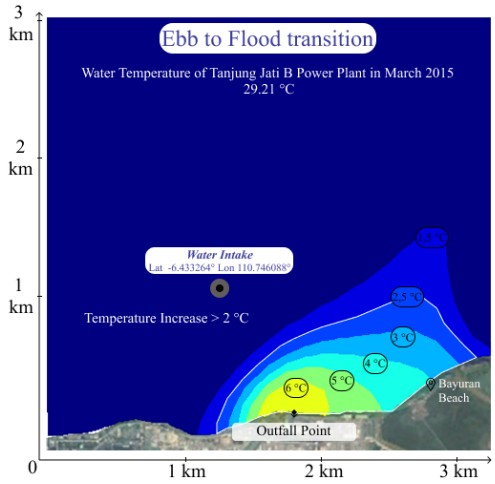

Figure 37. Increase in Thermal Water Temperature at Ebb to Flood Transisition Condition Compared to Ambient Water Temperature in 2015

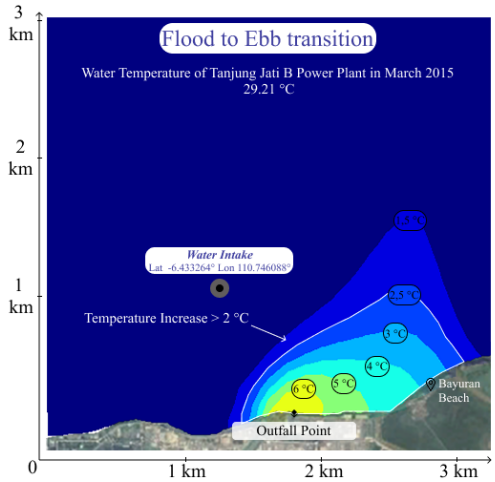

Figure 38. Increase in Thermal Water Temperature at Flood to Ebb Transition Condition Compared to Ambient Water Temperature in 2015

3. Average Temperature Variations

Figure 39 illustrates that the highest temperature increase during the lowest ebb condition reaches approximately ±8,5 °C. The area of seawater exhibiting a surface temperature rise greater than 2 degrees Celsius (> 2°C) around the power plant is approximately 1.450 m², with the maximum dispersion distance extending 1.630 meters from the outfall mouth. In contrast to the lowest ebb condition, Figure 40 shows that during the highest flood condition, the maximum temperature increase is about ±7,5 °C. The affected seawater area where the surface temperature increases by more than 2 °C is approximately 1.370 m², with a maximum dispersion distance of 1.545 meters.

Additionally, Figure 41 shows that during the ebb-to-flood transition, the highest temperature increase remains at

approximately ±8,5 °C. The area with a surface temperature rise exceeding 2 °C around the power plant is about 1.370 m², with the maximum plume extent reaching 1.570 meters from the outfall mouth. Similarly, in the flood-to-ebb transition condition (Figure 42), the peak temperature increase remains around ±8,5 °C, comparable to the ebb-to-flood condition. The area affected by a temperature increase exceeding 2 °C is approximately 1.255 m², with a maximum dispersion distance of 1.530 meters.

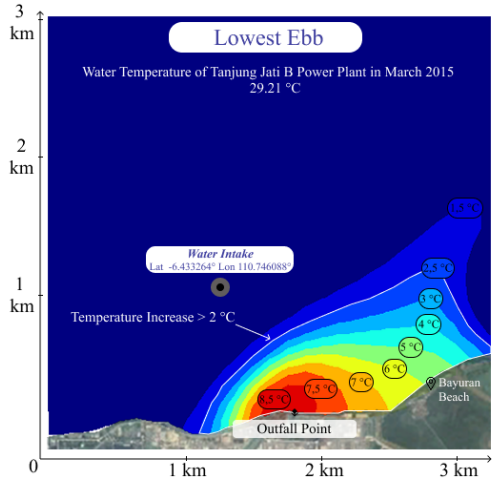

Figure 39. Increase in Thermal Water Temperature at Lowest Ebb Condition Compared to Ambient Water Temperature in 2015

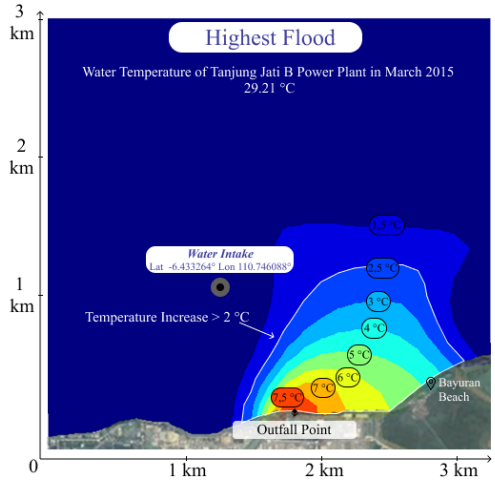

Figure 40. Increase in Thermal Water Temperature at Highest Flood Condition Compared to Ambient Water Temperature in 2015

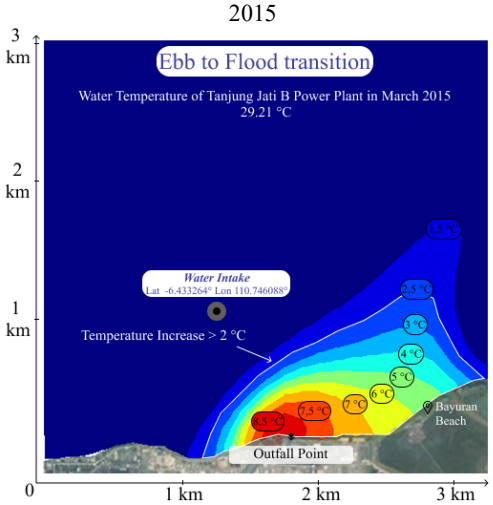

Figure 41. Increase in Thermal Water Temperature at Ebb to Flood Transisition Condition Compared to Ambient Water Temperature in 2015

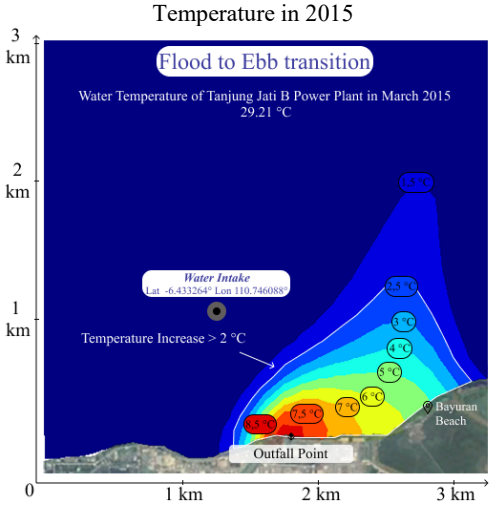

Figure 42. Increase in Thermal Water Temperature at Flood to Ebb Transition Condition Compared to Ambient Water Temperature in 2015

4.4.2 West Monsoon Condition (March)

1. Minimum Temperature Variations

In this simulation variation, no temperature changes were observed around the power plant, as the temperature difference between the ambient seawater and the outfall discharge was minimal, being less than 1 °C.

2. Average Temperature Variations

Figure 43 shows that the highest temperature increase under the lowest ebb condition is approximately ±5 °C. The area of seawater experiencing a surface temperature rise greater than 2 degrees Celsius (> 2°C) around the power plant is approximately 1.530 m², with the maximum dispersion distance extending 1.680 meters from the outfall mouth. Under the highest flood condition (Figure 44) the maximum temperature increase is approximately ±4 °C,

which is lower than that observed during the lowest ebb. The area affected by surface temperature increases exceeding 2 °C is about 721 m², with a maximum dispersion distance of 1.780 meters from the outfall. Notably, Figure 43 illustrates that during the lowest ebb condition, *the seawater intake area of the power plant experiences a surface temperature increase exceeding 2 °C.*

The temperature dispersion patterns during the ebb-to-flood and flood-to-ebb transitions are similar. In Figure 45, the highest temperature increase during the ebb-to-flood transition is about ±5 °C, with an affected seawater area of approximately 1.580 m² and a maximum dispersion distance of 1.820 meters from the outfall mouth. Similarly, Figure 46 shows that during the flood-to-ebb transition, the peak temperature increase remains around ±5 °C. The area experiencing a surface temperature rise over 2 °C is approximately 1.050 m², with the maximum extent reaching 1.700 meters from the outfall.

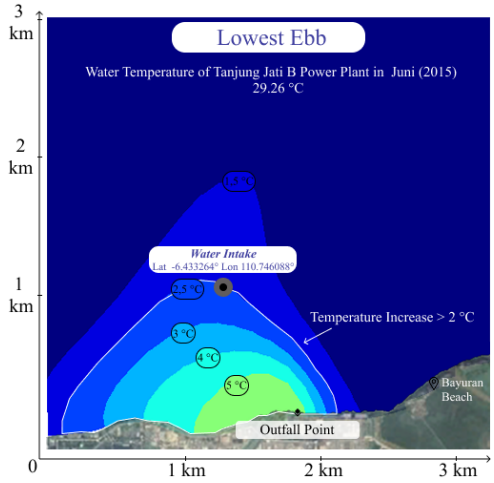

Figure 43. Increase in Thermal Water Temperature at Lowest Ebb Condition Compared to Ambient Water Temperature in 2015

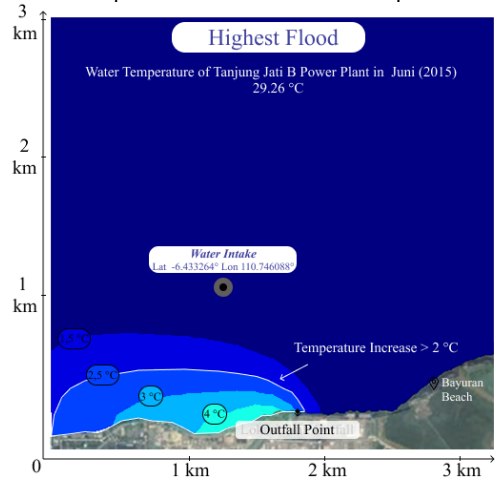

Figure 44. Increase in Thermal Water Temperature at Highest Flood Condition Compared to Ambient Water Temperature in 2015

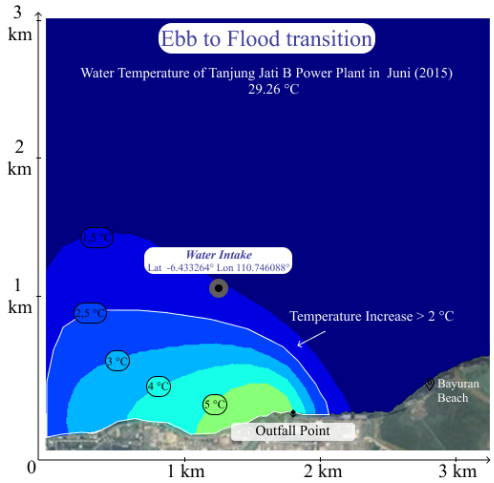

Figure 45. Increase in Thermal Water Temperature at Ebb to Flood Transisition Condition Compared to Ambient Water Temperature in 2015

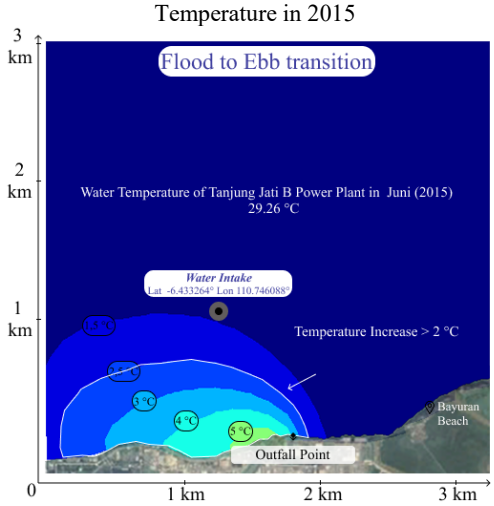

Figure 46. Increase in Thermal Water Temperature at Flood to Ebb Transition Condition Compared to Ambient Water Temperature in 2015

3. Average Temperature Variations

Figure 47 shows that the highest temperature increase during the lowest ebb condition reaches approximately ±9 °C. The area of seawater experiencing a surface temperature rise greater than 2 degrees Celsius (> 2°C) around the power plant is approximately 2.238 m², with the maximum dispersion distance extending 1.800 meters from the outfall mouth. In contrast, during the highest flood condition (Figure 48), the maximum temperature increase is approximately ±7.5 °C, with the affected area reduced to about 1.070 m², which is considerably smaller than that in the lowest ebb condition. The maximum dispersion distance during this condition is 1.850 meters from the outfall mouth. *Notably, at the lowest ebb, the water intake area experiences a temperature increase of up to 3 °C.*

Figure 49 illustrates the highest temperature increase during the ebb-to-flood transition at approximately ±9 °C. The affected seawater area, where surface temperature

increases exceed 2 °C, is approximately 2.152 m², with a maximum dispersion distance of 2.020 meters from the outfall mouth. Subsequently, Figure 50 (right) shows that during the flood-to-ebb transition, the peak temperature increase is about ±8.5 °C. The affected area measures approximately 1.560 m², with the maximum dispersion distance reaching 1.845 meters from the outfall mouth.

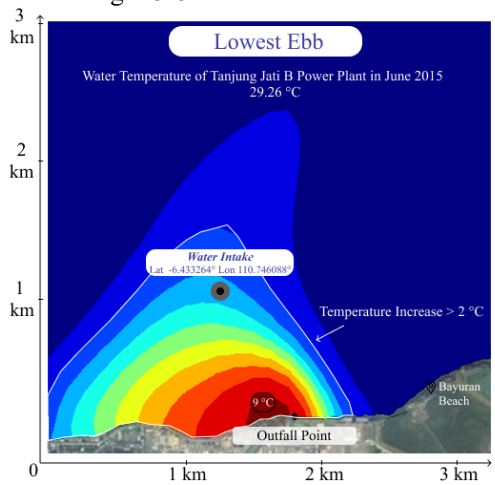

Figure 47. Increase in Thermal Water Temperature at Lowest Ebb Condition Compared to Ambient Water Temperature in 2015

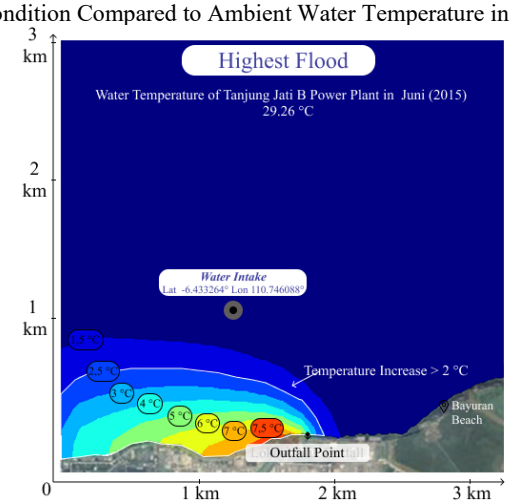

Figure 48. Increase in Thermal Water Temperature at Highest Flood Condition Compared to Ambient Water Temperature in 2015

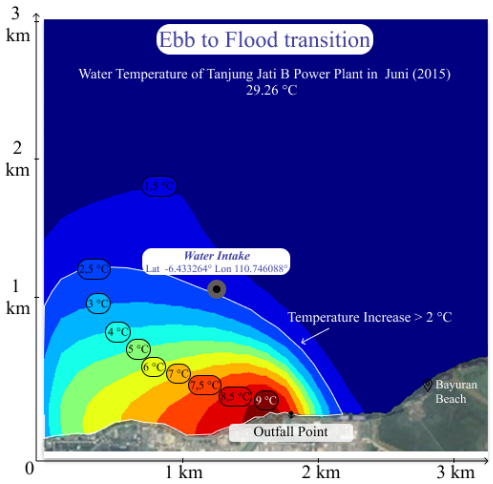

Figure 49. Increase in Thermal Water Temperature at Ebb to Flood Transisition Condition Compared to Ambient Water Temperature in 2015

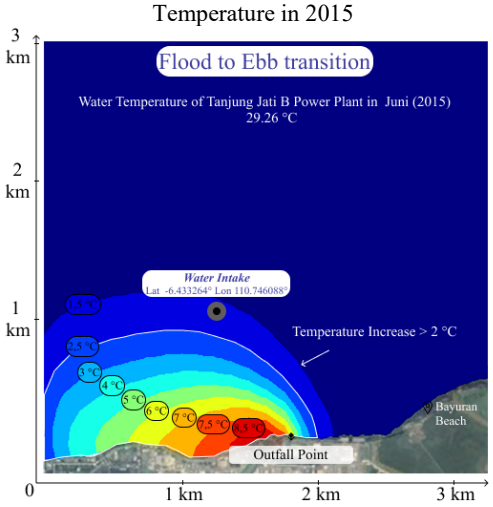

Figure 50. Increase in Thermal Water Temperature at Flood to Ebb Transition Condition Compared to Ambient Water Temperature in 2015

4.5 Identification of Solutions to Minimize the Dispersion Area of Waste Heat Discharge

Two indicative solutions have been identified to minimize the dispersion area of waste heat water temperature in the waters surrounding Tanjung Jati B Power Plant units 5 and 6. A brief overview is provided below.

1. Modification of the Existing Outfall Channel Bed Design for PLTU Tanjung Jati B Units 5 & 6

This solution involves redesigning the channel bed to avoid a flat bottom profile. According to Zheng et al. (2023) [8], introducing variations that disrupt fluid flow and prevent laminar conditions can accelerate the cooling of water temperature. Their study conducted simulations of open channel flows with varied bed shapes, demonstrating

temperature reductions ranging from 9% to 22.5% across all simulation scenarios. Therefore, modifying the outfall channel bed to be rougher, thereby inducing more turbulent flow, is a viable solution worth considering to enhance thermal dissipation.

2. Implementation of a Spray Pond System on the Existing Outfall Channel

A simple and relatively low-cost method is the use of a spray pond. Spray ponds function by ejecting water into the air, facilitating evaporation and enhancing convective heat transfer from the water to the atmosphere in a relatively straightforward and economical manner. According to Ananda et al. (2017) [9], spray ponds exhibit higher effectiveness compared to conventional cooling towers. Spray ponds achieve an efficiency of 93.75%, reducing water temperature from 45 °C to 30 °C, whereas conventional cooling towers reach only 75% efficiency, lowering temperatures from 45 °C to 33 °C.

5. CONCLUSIONS

The conclusion of this study indicates that the dispersion pattern of waste heat discharge during the West Monsoon predominantly trends toward the northeast, whereas under the East Monsoon, the dispersion tends to be directed toward the west, northwest, and north. Furthermore, the four tidal phases exert a significant influence on the dispersion pattern of waste heat, with the lowest ebb condition exhibiting the widest and most extensive thermal plume area, while the highest flood condition corresponds to the smallest and most confined dispersion zone. These results demonstrate that ocean currents, wave dynamics, and tidal timing collectively play critical roles in shaping the distribution of waste heat discharge.

Additionally, the study reveals that the thermal impact of waste heat discharge significantly alters the seawater temperature surrounding the power plant. The highest observed temperature increase reaches up to 9 °C, with an average affected area—where temperature increases exceed 2 °C—measured at 932.16 m² during the West Monsoon and 1,487.62 m² during the East Monsoon, based on 2024 dispersion patterns compared to baseline water temperatures in 2015. Notably, in several conditions, temperature increases exceeding 2 °C were detected within the water intake area, which holds critical importance for the operation of PLTU Tanjung Jati B units 5 and 6.

These findings underscore the necessity for continuous monitoring and effective management strategies to mitigate thermal impacts and ensure the sustainable operation of the power plant in relation to the surrounding marine environment.

REFERENCES

[1] Syahputra, R. (2020). TEKNOLOGI PEMBANGKIT TENAGA LISTRIK.

[2] Awliya Muhammad Ashfania, G., Haryanto, I., & Awliya Muhammad Salman, H. (2021). Optimisasi Dimensi Kanal Outfall Air Pendingin PLTU Dengan Memperhatikan Dampak Lingkungan Pada Air Laut (Vol. 23, Issue 3).

[3] Lanuru, M. (2022). Model Sebaran Thermal Air Pendingin PLTU dan Kaitannya Dengan Komposisi Jenis Plankton dan Benthos Di Perairan Biringkassi. Proceeding of International and National Conference on Marine Science and Fisheries, 299–305.

[4] Darwis, I., Dwiyanto, M., Prakasa, A., & Amansah, S. (n.d.). Analisis Penurunan Suhu Air Limbah PLTU Menggunakan Cooling Water Way pada PLTU Jeneponto 2X125MW Analysis of Reducing the Temperature of Steam Power Plant Waste Water Using Cooling Water Way PLTU Jeneponto 2X125 MW. In Journal of Applied Civil and Environmental Engineering (Vol. 3, Issue 2).

[5] Permadi, L. C., Indrayanti, E., & Rochaddi, B. (2015). STUDI ARUS PADA PERAIRAN LAUT DI SEKITAR PLTU SUMURADEM KABUPATEN INDRAMAYU, PROVINSI JAWA BARAT. 4(2), 516–523. http://ejournal-s1.undip.ac.id/index.php/jose

[6] Wara, A. D. (2019). Costal Protection. https://www.researchgate.net/publication/332738614

[7] Ghilani, C. D.., & Wolf, P. R. (2006). Adjustment computations spatial data analysis. John Wiley & Sons.

[8] Zheng, S. F., Liu, G. Q., Zhang, Y., Wang, H. C., Gao, S. R., Yang, Y. R., Li, H. W., Sunden, B., & Wang, X. D. (2023). Performance evaluation with turbulent flow and heat transfer characteristics in rectangular cooling channels with various novel hierarchical rib schemes. International Journal of Heat and Mass Transfer, 214. https://doi.org/10.1016/j.ijheatmasstransfer.2023.124459

[9] Santhosh Ananda, C. P., Sekar, N., Kumar, S. S., Sheik Hyder, S., & Vignesh, S. (2017). Study of Cooling Towers and Comparision of Conventional Cooling Tower and Spray Cooling Pond. www.ijert.org